Available online at www.sciencedirect.com
SCIENCE DIRECT
Polymer 46 (2005) 5241–5250
polymer
www.elsevier.com/locate/polymer

Crystallisation of polypropylene containing nucleators

Shinta Nagasawa[1], Atsuhiro Fujimori, Toru Masuko, Masatoshi Iguchi*

Department of Polymer Science and Engineering, Faculty of Engineering, Yamagata University, Yonezawa 992-8510, Japan

Received 15 June 2004; received in revised form 7 March 2005; accepted 28 March 2005
Available online 5 May 2005

Abstract

The crystallisation of polypropylene in the presence of sodium benzoate, graphite powders, Millad 3988 (1,3:2,4-*bis*(3,4-dimethylbenzylidene sorbitol)) and NA-11 (sodium 2,2′-methylene *bis*-(4,6-di-*tert*-butylphenyl)phosphate) was studied. As a parameter for the effectiveness of nucleators, a free-energy parameter for the nucleation was estimated, on the basis of a theory, from the nucleation temperature during cooling at various rates. The density of actual nuclei was estimated from the radial growth rate of spherulites and the bulk growth rate, the latter obtained by the analysis of crystallisation isotherms. The dispersibility of nucleator particles calculated with reference to the mean volume of particles was various, the cluster size being ranged between unity to several hundred. The Young's modulus of films prepared from the polymer–nucleator mixtures has been found to correlate with the nucleus density without respect to the kind of nucleator.

Keywords: Polypropylene; Crystallisation; Nucleator

1. Introduction

Ever since polyacetal resin was first commercialised in early 1960s, various engineering plastics have become available, being applied to a wide range of commodity products, as one sees them today. Although the development owes primarily to the achievement of the synthesis of new polymers such as polyolefines, polyphenols, polysulphone and aromatic polyamides, the application of various additives as well as the advance in moulding technology has played an important role.

For some crystalline polymers, the addition of nucleator is significant for modifying the fine structure and improving the physical properties of the products. Particularly for isostatic polypropylene which normally forms large spherulites from the melt, it is a benefit that the increase in the density of nuclei, and hence the decrease in the diameter of spherulites below the wavelength of visible light, improves the transparency of moulds, whilst the shortening of processing time and some improvement of mechanical properties are bonuses. For this purpose, powders of various compounds such as sodium benzoate, sorbitol derivatives and organophosphate salts have been developed and of common use (see, brochures of Milliken and Co., Asahi Denka Co. Ltd, etc). Graphite would have a potentiality to be a nucleator, on account of the fact that polypropylene and other polymers crystallised epitaxially on highly graphatised carbon fibre (Watanabe and Iguchi [1]), although its effect on the optical property is quite contrary and the colour of the polymer has to be blackened. While various substances are thus of interest, it is common that their effect is judged for individual substance, more or less on try-and-error basis, from the properties of resultant moulds.

The primary factor which determines the effectiveness of a nucleator is the interfacial free-energy between the polymer and the nucleator particles, and a theoretical method to estimate a free-energy parameter from DSC (differential scanning calorimetry) traces under constant-rate cooling was proposed earlier by one of the present authors (Iguchi and Watanabe [2,3]) and applied to polyoxymethylene whisker/polyacetal and graphite fibre/polypropylene systems (Watanabe and Iguchi [1]), whereas a different approach was made recently for the

* Corresponding author. Present address: Visiting Professor, Department of Chemical Engineering and Chemistry, Eindoven Technical University, 5612 A2 Eindhoven, The Netherlands. Fax: +31-40-243-6999.
E-mail address: maiguch@attglobal.net (M. Iguchi).
[1] Present address: Brucker AXS K.K., Kanagawa, Yokohama 2210022, Japan.

0032-3861/$ - see front matter © 2005 Elsevier Ltd. All rights reserved.
doi:10.1016/j.polymer.2005.03.099

Nomenclature

General

ΔH_u	heat of fusion (J m^{-3})
κ_B	Boltzman constant (J K^{-1})
T_m^0	equilibrium melting temperature (K)
T_m	melting temperature (K)

Nucleation

α	a free energy parameter of critical nucleus (J)
$\phi(u)$	nucleation frequency as a function of under-cooling, u (K^{-1})
K_v	a kinetic factor for molecular transportation (m^{-3} s^{-1})
r	the rate of cooling $= -du/dt$ (K s^{-1})
σ_{xy}, σ_{yz}, σ_{zx}	surface free energy of three sectors of an orthorhombic primary nucleus (J m^{-2})
σ_{o-zx}	surface free energy of $z-x$ sector of an orthorhombic primary nucleus in contact with the nucleator surface (J m^{-2})
u	under-cooling (super-cooling) $= T_m^0 - T$ (K)
v_d	average volume of polymer to be frozen at the time of nucleation (m^3)
W^*	volume free energy to form a critical nuclei (J)
$\Psi(u)$	integral of $\phi(u')$ from $u'=0$ to $u'=u$ (Eq. (2)) (−)

Isothermal crystallisation

b	the thickness of mono-molecular layer (cm)
C	number of nuclei (simultaneous nucleation) (m^{-3})
c_i	number of nuclei activated at time, t_i (m^{-3})
g	radial growth rate of spherulite (m s^{-1})
K	volume crystallisation rate $= C(4\pi/3)g^3$ (s^{-3})
N	the number of nucleator particles (m^{-3})
σ_e, σ_s	end- and side-surface free energy of secondary nucleus (J m^{-2})
T_c	crystallisation temperature (K)
ΔT	under-cooling (super-cooling) $= T_m^0 - T_c$ (K)
V	volume fraction transformed by a certain time (−)
V_{free}	total volume of spherulites when no impingement assumed (relative to the unit volume) (−)
V_∞	transformable volume fraction (−)
X	transformed volume fraction or the degree of crystallisation (−)

analysis of DSC traces for dibenzilidene sorbitol/polypropylene system (Feng et al. [4]). The dispersibility, or the degree of clustering of nucleator particles in the polymer melts, must be also important because it determines the actual nucleus density in polymer–nucleator mixtures. Qualitatively, it can be evaluated by microscopic observation but the method is not necessarily suitable to elucidate the state of distribution in thick moulds. Recently, the density of nuclei in polypropylene containing various amount of an organophosphate salt has been estimated (by Kim and Kim [5] and Gui et al. [6], respectively) on a non-isothermal crystallisation kinetic equation, and the relationship between the nucleation mechanical properties, investigated, but the dispersibility of particles has not been concerned.

This paper reports some results on the crystallisation of polypropylene to which various nucleating substances such as sodium benzoate, a sorbitol derivative, an organophosphate salt and graphite powders were added. Specifically, a free-energy parameter for nucleation has been evaluated by the former method (Iguchi and Watanabe [2,3]). The density of actual nuclei has been estimated in a direct manner from the radial growth rate of spherulites measured under the optical microscope and the bulk growth rate obtained by the analysis of crystallisation isotherms, and the dispersibility of nucleator particles, calculated with reference to the mean volume of particles. The Young's modulus of film specimens prepared from the polymer–nucleator mixtures have been found to correlate with the nucleus density without respect to the kind of nucleator.

2. Experimental

2.1. Materials

Polypropylene employed for this study was E-200GP ($M_w = 4.42\times10^5$, $M_w/M_n = 4.38$) from Idemitu Petrochemical Co. Substances chosen as nucleators were sodium benzoate (from Asahi Denka Co.), graphite powders of two different grades (SP-270 and T1 from Nippon Graphite Industry Co.), a sorbitol derivative (1,3:2,4-*bis*(3,4-dimethyl-benzylidene sorbitol), Millad 3988, from Milliken Co.), and an organophosphate salt (sodium 2,2′-methylene *bis*-(4,6-di-*tert*-butylphenyl)phosphate, NA-11, from Asahi Denka Co). To characterise the shape and the size of nucleators, scanning electron-micrographs (SEM) were taken with a JSM-5300, of JEOL Ltd.

The polymer mixed with each nucleator was kneaded at 210 °C for 15 min by means of a Labo-Plastomil, of Toyoseiki Co. The specifications of samples prepared are shown in Table 1.

Table 1
Polypropylene–nucleator mixtures prepared for this study

Code	Nucleator	Content (wt%)
PP		
PP-NaBz	Sodium benzoate	0.1
PP-SP	Graphite (SP-270)	0.1
PP-T1	Graphite (T1)	0.1
PP-Mi	Millad 3988	0.1
PP-NA0.1	NA-11	0.1
PP-NA0.05	NA-11	0.05

2.2. Optical microscopy

A polarising microscope, BH-5, of Olympus Corp., equipped with a hot-stage, TMH-600, of Linkam Scientific Instruments Ltd, was used. For the measurement of the radial growth rate of spherulites in isothermal conditions, molten polypropylene was cooled rapidly at the rate of 130 °C/min (machine setting), and kept at preset temperatures (124–128 °C). Photographs were taken at 0.5–1.0 min intervals, and the radius was measured for 40–60 spherulites.

2.3. Differential scanning calorimetry (DSC)

A Pyris1 of Perkin Elmer, Inc. was used. For the determination of the nucleation temperatures, or the starting temperature of crystallisation exotherm during cooling, samples were molten at 210 K for 5 min and the temperature was lowered at various rates, 0.31–40 K/min. For obtaining the crystallisation isotherms to analyse the bulk growth rate, the temperature was lowered at 80 K/min (machine setting) down to the preset crystallisation temperature (124–140 °C) and maintained until the exotherm returned to the baseline.

For both cases, the analysis of data was conducted on home-made programmes specially written for these purposes.

2.4. Tensile test

Films were prepared by the heat-press method in which the pressed polymer was left sandwiched in the machine until the temperature went down below 90 °C to complete the crystallisation. For the measurement, a tensile tester, AG-5kNE of Shimadzu Corp., was used. The measurement was carried out for specimens of 3 mm wide × 40 mm long (distance between the chucks) at room temperature (20 ± 1 °C) at the elongation speed of 25%/min. To obtain the data in an accurate digital form, a voltmeter having a RS232 port was devised and the data was transferred into a computer using a specially written programme. The analysis of Young's modulus from the stress–strain curves was performed with another home-made programme.

3. Results and discussion

3.1. Characterisation of nucleator powders

Fig. 1 shows the SEM of nucleators. The shapes of particles were simulated with simple shape models and the sizes were measured for 60–100 pieces. The size distribution of particles are shown in Fig. 2 and the mean sizes and the mean volumes, summarised in Table 2.

3.2. Confirmation of spherulitic morphology and the measurement of radial growth rate

Whilst the neat polypropylene sample yielded a typical spherulites from the melt, with negative birefringence, the size of spherulites turned to be very minute by the addition of nucleators as seen in the polarised micrographs in Fig. 3, demonstrating that the additive particles had really furnished nucleus. The appearance of spherulites was observed within a short time, and accordingly their sizes were homogeneous, implying that the activation of nuclei had taken place within a short period. This was true even for the neat polymer, suggesting that a small amount of some impurities, presumably the residue of some catalyst existed in the original polymer, had acted as a 'natural' nucleator.

For the neat polymer, isothermal crystallisation was conducted under the polarised microscope at preset temperatures, 124–128 °C, and the radius of spherulites was followed as shown in Fig. 4. The birth of spherulites concentrated in a short time range, and the diameters increased linearly with virtually equal slopes. The growth rate, g, calculated from the slope and the nucleation time obtained from the intercepts of fitted lines on the time axis are summarised in Table 3.

Although the standard deviation of nucleation time as well as the time itself tended to be larger as the crystallisation temperature was higher, the magnitude remained relatively small (<2 min) compared with the total crystallisation time (>30 min). For samples mixed with nucleators, numerous spherulites appeared all at once in the dark field under polarised microscope when the temperature reached the preset crystallisation temperatures, making the measurement of radius technically difficult. Also in experiments conducted under constant rate cooling, the appearance of spherulites or the activation of nuclei looked almost 'simultaneous'.

3.3. Nucleation free energy

Theories relating to the crystal nucleation as well as the crystallisation in polymer systems was developed decades ago when various crystalline polymers emerged (Mandelkern [7]). The following approach is based on a work accomplished by one of the present authors (Iguchi and Watanabe [2,3]).

The distribution of nucleation frequency, $\phi(u)$ as a function of the under-cooling u, is related to the volume free energy to form a critical nucleus, W^* (Burns and Turnbull [8]). If the transformed volume fraction, X is small at the stage of nucleation,

$$r\phi(u) = K_v v_d \exp\left[\frac{-W^*}{\kappa_B(T_m^0 - u)}\right][1 - \psi(u)] \quad (1)$$

where κ_B is the Boltzmann constant, K_v is a kinetic factor for

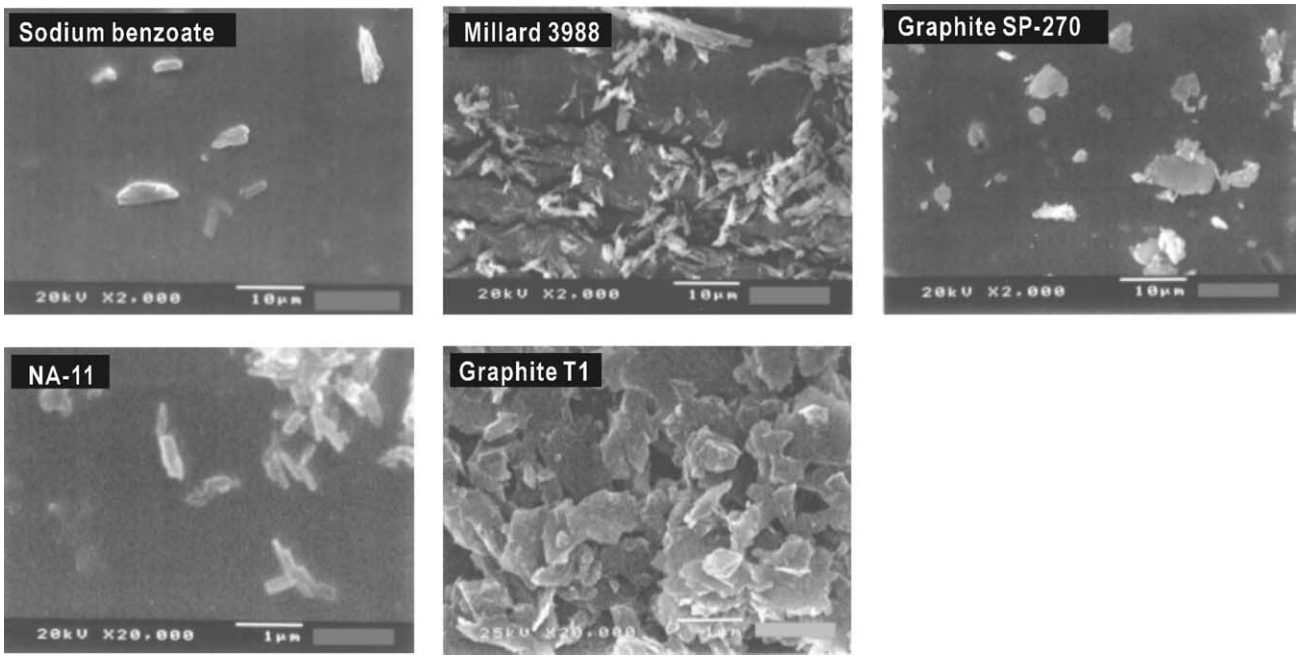

Fig. 1. Scanning electron-micrographs of nucleators.

molecular transportation and v_d is the average volume of polymer to be frozen (or, in Burns and Turnbull's term, the average volume of 'droplets'),

$$\psi(u) = \int_0^u \phi(u')\mathrm{d}u' \tag{2}$$

and

$$W^* = \alpha\left(\frac{T_m^0}{u}\right)^2 \tag{3}$$

Here, α is the parameter relating to the form of critical nucleus and the mode of nucleation. For instance, if an 'orthorhombic' nucleus as shown in Fig. 5 is assumed, the parameter takes the form of,

$$\alpha_{\mathrm{free}} = \frac{32\sigma_{xy}\sigma_{yz}\sigma_{zx}}{\Delta H_u^2} \tag{4}$$

and

Table 2
Shape model and size of nucleators

Substance	Nucleator			
	Shape model	Mean size (μm)	Density (g/cm^3)	Mean volume[a] (μm^3)
Sodium benzoate	Spheric	$d=2.35$	1.44	16.0
Graphite (SP-270)	Discoidal	$d=2.72$, $h=0.432$	2.25	2.51
Graphite (T1)	Discoidal	$d=0.389$, $h=0.0322$	2.25	3.83×10^{-3}
Millad 3988	Tetragonal	$a=1.06$, $c=3.23$	0.725	4.54
NA-11	Tetragonal	$a=0.239$, $c=0.547$	1.18	5.61×10^{-2}

[a] The mean volumes for the spheric, discoidal and tetragonal particles were calculated by: $\sum_{i=1}^{\infty} n_i(4/3)\pi r_i^3/\sum_{i=1}^{\infty} n_i$, $\sum_{i=1}^{\infty} n_i(\pi r_i^2 d_{av})/\sum_{i=1}^{\infty} n_i$ and $\sum_{i=1}^{\infty} n_i(a_i^2 c_{av})/\sum_{i=1}^{\infty} n_i$, respectively.

Table 3
Radial growth rate of spherulites

Crystallisation temperature, T_c (°C)	Radial growth rate, g (μm/min)	Mean nucleation time (min)	Standard deviation of nucleation time (min)
124	27.7 ± 1.90	0.44	0.40
125	19.8 ± 1.17	0.64	0.96
126	16.3 ± 1.04	0.85	1.56
127	12.8 ± 0.84	0.91	1.18
128	11.1 ± 0.61	1.62	1.63

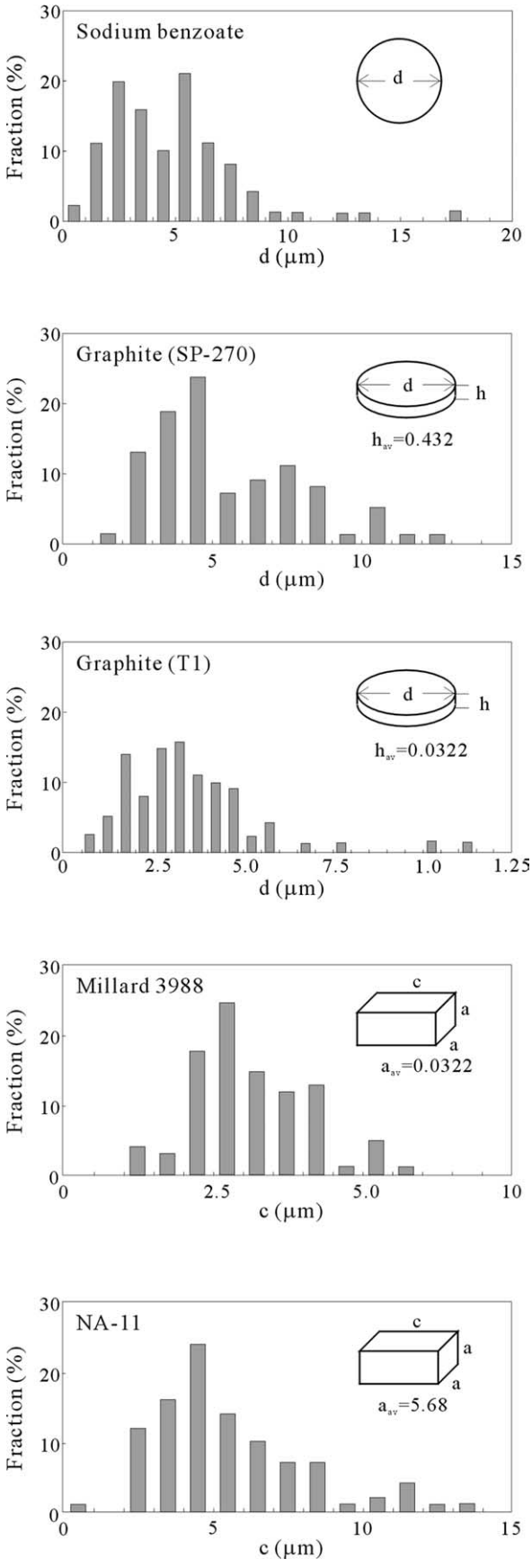

Fig. 2. Size distribution of nucleator particles.

$$\alpha_{\mathrm{surf}} = \frac{16\sigma_{xy}\sigma_{yz}(\sigma_{zx} - \sigma_o + \sigma_{o-zx})}{\Delta H_{\mathrm{u}}^2} \tag{5}$$

for the free- and surface-nucleations, respectively.

By replacing Eq. (3) into Eq. (1),

$$ar\phi(u) = K_{\mathrm{v}} v_{\mathrm{d}} \exp\left[\frac{\alpha T_{\mathrm{m}}^{0^2}}{\kappa_{\mathrm{B}}(T_{\mathrm{m}}^0 - u)u^2}\right][1 - \psi(u)] \tag{6}$$

Differentiating Eq. (6) by u and setting $\phi'(u)=0$ to find the maximum of $\phi(u)$, followed by arranging, one obtains

$$-\ln\left[\frac{r(2T_{\mathrm{m}}^0 - 3u)T_{\mathrm{m}}^{0^2}}{(T_{\mathrm{m}}^0 - u)^2 u^3}\right]$$

$$= \frac{(\alpha/\kappa_{\mathrm{B}})T_{\mathrm{m}}^{0^2}}{(T_{\mathrm{m}}^0 - u)u^2} - \ln[(\kappa_{\mathrm{B}}/\alpha)K_{\mathrm{v}} v_{\mathrm{d}}] \tag{7}$$

Thus, the value of $\alpha/\kappa_{\mathrm{B}}$ can be obtained from the slope of the plot on Eq. (7), if the undercooling, u, at maximum $\phi(u)$ is available.

From the microscopic observation, $\phi(u)$ can be regarded to be very narrow. Then, u at maximum $\phi(u)$ was represented as first approximation by the temperature at which the crystallisation exotherm was discerned on the DSC traces.

Fig. 6 shows examples of DSC traces obtained at various cooling rates. For both PP and PP-NA0.1, i.e. the neat sample and one of the nucleator-added samples, the change of curves was quite systematic, being moved to the lower temperature side and broadened as the cooling rate increased. The set of curves of the nucleator-added sample were shifted to the higher temperature side, demonstrating the effect of the nucleator. The values of undercooling, calculated from the temperatures at which the curves took off the baseline and the equilibrium melting temperature, 495.5 K (Kamide [9]), are summarised in Table 4.

The data plotted according to Eq. (7) were reasonably linear as shown in Fig. 7. It is remarked that the points of PP-SP and PP-T1 appeared almost on the same line, proving that the effect of graphite as a nucleator, in terms of the free energy, was consistent regardless to the particle size. It should be noted that the total crystallisation process is governed also by the density of nuclei and the rate of PP-T1 is much faster than that of PP-SP (for isothermal crystallisation, the density of nuclei was estimated as in Table 7).

It is also interesting that the slopes of PP-Na0.05 and PP-Na0.1, containing the same nucleator but in different contents, are virtually the same. The slope of PP-NaBz was a little smaller than that of neat PP, implying that the surface free-energy of sodium benzoate was only a little lower than that of the 'natural' nucleator contained in the original polymer. The plots of PP-Mi are overlapped with those of PP (neat), suggesting that Millad 3988 had little effect for the present polypropylene. The values of V_∞ obtained from the slopes and the Boltzmann constant are shown in Table 5.

For polypropylene of a different origin (Scientific Polymer

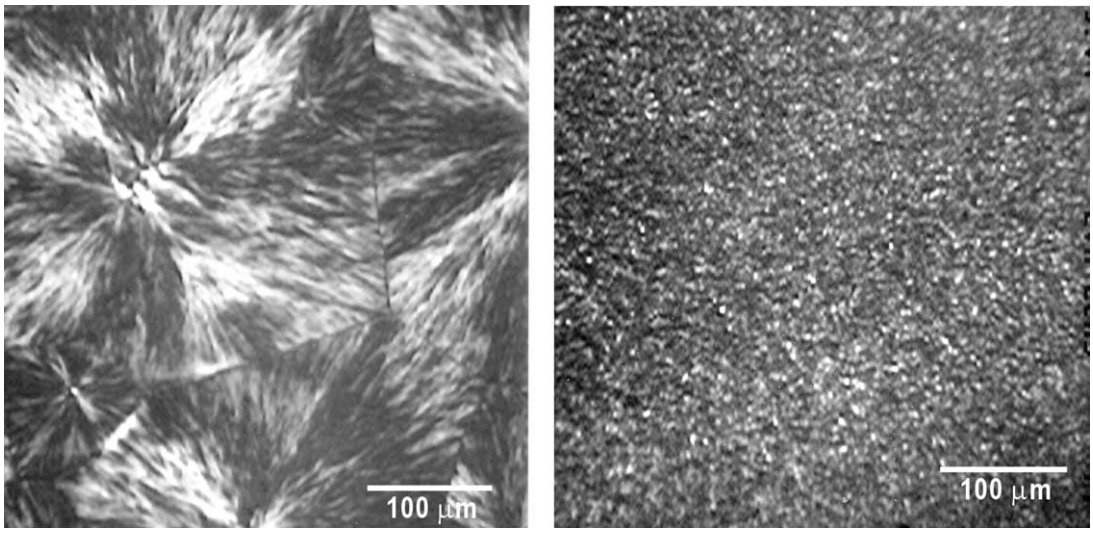

Fig. 3. Polarised micrographs of spherulites grown during cooling at 5 K/min from the melt (210 °C). Left: PP (neat), right: PP-NA0.1.

Products, Inc.; #130, inherent viscosity = 2.2–2.5), the value of V_∞ obtained by the same measurement and analysis was 11.05×10^{-22} J, agreeing well with that of the present polymer, 11.07×10^{-22} J. The old data for polypropylene and graphite fibre-embedded polypropylene (Watanabe and Iguchi [1]) were 4.52×10^{-22} and 2.87×10^{-22} J, respectively, being much different from the present results. Since, not only the value for the nucleation of neat polymer but also the same for the nucleation on graphite surface is different and much smaller, it is supposed that some properties of the polymer at that age would have been different.

3.4. The nucleus density and the cluster size of nucleator particles

Whilst some modified or new theories have been proposed for the kinetics of crystallisation in bulk system (e.g. Banks et al. [10], Hillier [11], Danusso et al. [12]) for the kinetics of crystallisation in bulk system, the Avrami–Evans theory (Avrami [13] and Evans [14]) is still useful at least when a well defined growing bodies grows in an isothermal condition, as has been studied and verified in early days (Mandelkern [7]), and successfully applied to the spherulite and cylindrite growths of polyoxymethylene crystals (Iguchi and Watanabe [3]). This was also true for polypropylene (Kamide [8], Iguchi and Watanabe [1]) contrary to some controversial statements found in literature (Kim and Kim [5], Gui et al. [6]). For the present purpose to estimate the density of nuclei in particular, the use of the classic theory is advantageous because the only other parameter required is the radial growth rate of spherulite which can be directly measured by microscopic method.

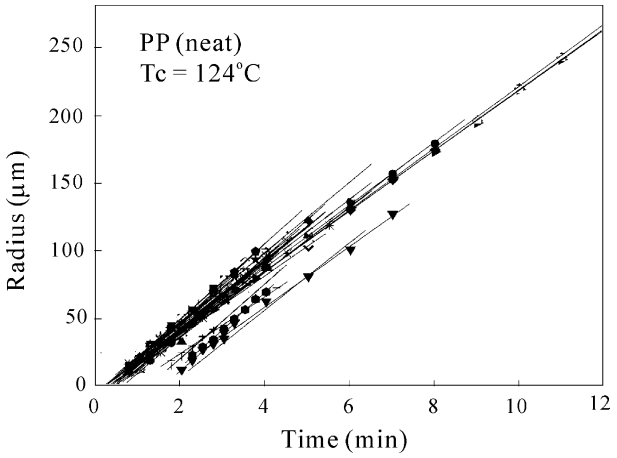

Fig. 4. Radii of spherulites plotted vs. time (T_c = 120 °C).

If spherulites are assumed to grow in a free space without impingement, the total volume relative to the unit volume transformed by time, t is given by,

$$V_{\text{free}} = \sum_{i=1}^{\infty} c_i \left(\frac{4\pi}{3}\right)[g(t-t_i)]^3 \tag{8}$$

where, c_i is the number of nuclei per unit volume activated at time, t_i, and g is the radial growth rate. If the mode of nucleation is 'simultaneous', as in the present case,

$$V_{\text{free}} = C\left(\frac{4\pi}{3}\right)(gt)^3 \tag{9}$$

where C is the total density of nuclei.

For the real space in which a number of spherulites

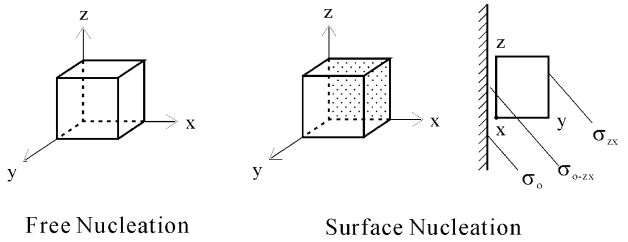

Fig. 5. A model for 'orthorhombic' primary nucleus.

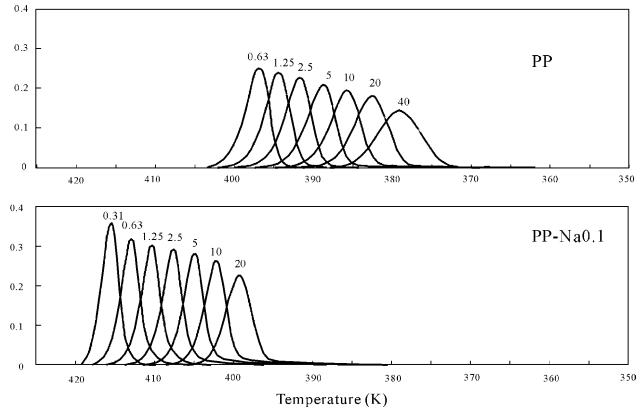

Fig. 6. Examples of DSC crystallization traces during cooling at constant rates (normalised). The figures above peaks indicate the cooling rates in K/min.

collides with each other and their growth is restricted, the Avrami–Evans theory teaches,

$$1 - \frac{V}{V_\infty} = \exp(-V_{\text{free}}) \tag{10}$$

where, V_∞ is the transformable volume fraction and V is the volume fraction transformed by a certain time.

By representing V/V_∞ by the degree of crystallisation, X, and replacing Eq. (9),

$$1 - X = \exp(-Kt^3) \tag{11}$$

or

$$\log[-\ln(1 - X)] = \log K + 3\log t \tag{12}$$

where,

$$K = C\left(\frac{4\pi}{3}\right)g^3 \tag{13}$$

From Eq. (13), the nucleus density, C may be estimated, if the bulk crystallisation rate, K can be obtained by the analysis of isothermal crystallisation data, with reference to the linear growth rate g, from microscopic measurement.

As established earlier (Kamide and Fujii [15]), DSC is a convenient method to follow the change of crystallinity as long as the exotherm is assumed to be proportional to the change of the crystallinity, dX/dt. Fig. 8 shows the DSC traces and their integrated curves obtained for PP-SP at various crystallisation temperatures. As seen in Fig. 9, the double-logarithm plots fitted well to straight lines, the slopes of which being very close to 3, in accordance with the assumptions that the occurrence of nucleation was simultaneous and the mode of the growth was three-dimensional. The result was in common with other samples, as summarised in Table 6 in which the values K and X_{peak}, i.e. the degree of crystallinity at maximum dX/dt, are also included. The latter values are close to the unique value, 48.66%, theoretically derived from Eq. (11) for the three-dimensional growth (Iguchi and Watanabe [2]).

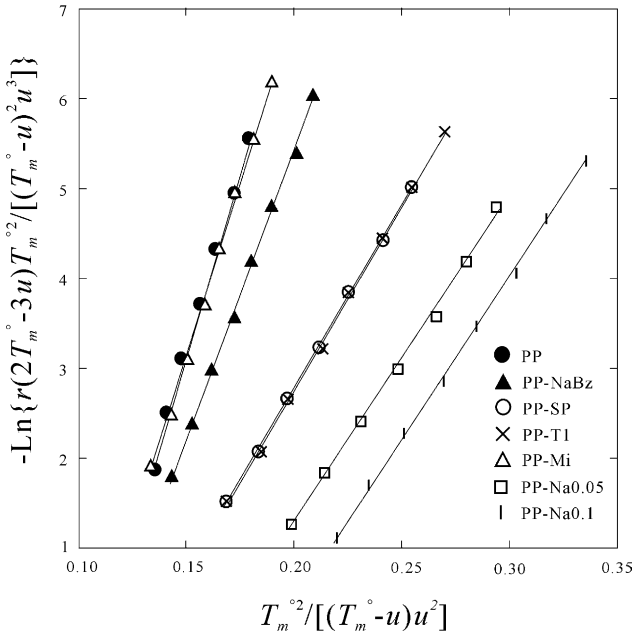

Fig. 7. Plot of nucleation under-cooling data in accordance with Eq. (7).

In Fig. 10, the values of (1/3)ln(K) and ln(g) are plotted against $T_c\Delta T$, on account of the equation for lamellar crystal growth (Mandelkern [7]), for which a 'secondary' nucleation is assumed as the source mechanism,

$$\ln g = A - \left(\frac{4\sigma_e\sigma_s b}{\kappa_B \Delta H_u}\right)\left(\frac{T_m^0}{T_c\Delta T}\right) \tag{14}$$

where T_m^0 is the equilibrium melting temperature, ΔT ($=T_m^0 - T_c$), the under-cooling, ΔH_u, the heat of

Table 4
Nucleation undercooling, u of polypropylene–nucleator mixture in the course of constant-rate cooling

Heating rate (K/min)	PP (neat)	PP-NaBz	PP-SP	PP-T1	PP-Mi	PP-NA0.1	PP-NA0.05
40	65.0	63.0	57.7	57.7	65.5	50.1	52.9
20	63.6	60.9	55.2	55.0	63.1	48.4	50.8
10	61.9	59.0	53.1	53.1	61.3	46.7	48.8
5	60.0	57.0	51.1	50.9	59.7	45.0	47.0
2.5	58.6	55.7	49.4	49.5	58.3	43.7	45.3
1.25	57.0	54.2	47.7	47.7	56.9	42.3	44.1
0.63	55.8	52.6	46.4	46.3	55.4	41.3	43.0
0.31		51.5		45.0	54.1	40.1	

$u = T_m^0 - T_i$, $T_m^0 = 495.5$. T_i, the temperature at which a DSC curve takes off the baseline.

Table 5
Free-energy parameters of nucleators

Substance	α ($\times 10^{-22}$ J)
'Natural' nucleator in the original polymer	11.07
Sodium benzoate	8.86
SP-270 (graphite; 3.23 μm)	5.59
T1 (graphite; 0.389 μm)	5.64
Millad 3988 (sorbitol derivative)	10.56
Na-11 (organophosphate compound)	4.94, 4.99[a]

[a] Results of two different contents, 0.05 and 0.1%.

transformation, b, the mono-molecular layer thickness, and σ_e and σ_s are the end and the surface energies.

Since, the data of ln(g) did not cover the whole range of (1/3)ln(K), some method to extrapolate the data was necessary. Although the slopes for the sets of points were not quite the same, their average value, −8.56, was adopted to draw the parallel lines. The values of C calculated from the difference along the vertical axis are shown in the second column of Table 7. There, N in the first column is the number of nucleator particles calculated from the size distribution in Fig. 2 along with the density of nucleator in Table 2 and the content of the nucleator. The ratio, N/C, in the last column are regarded as the degree of aggregation or the size of clusters. It is interpreted that, for instance, the dispersibility of sodium benzoate are rather poor and about 750 particles are considered to be clustered together. It is interesting that the cluster size for PP-SP is close to unity, implying that the particular carbon powder are very well dispersed, whereas the same for PP-T1 with another carbon powder of smaller size is somewhat larger and about 200. In PP-Na0.05 and Na0.1, the organophosphate powder is considered to be well dispersed, although the N/C value for the latter is a little smaller than unity due presumably to the inaccuracy in the size and the size distribution measurement

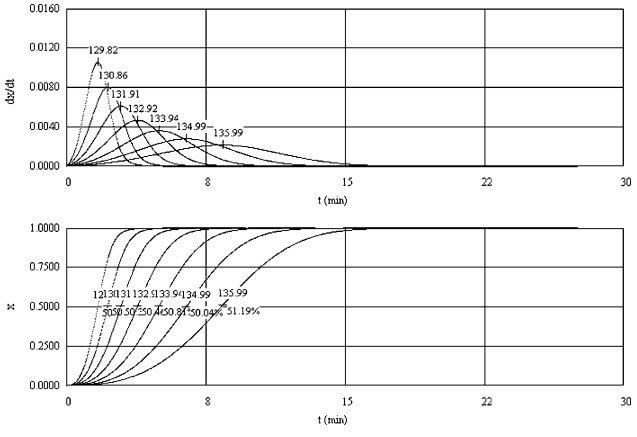

Fig. 8. Normalised DSC isotherms and their integrated curves of PP-SP at various crystallisation temperatures. The figures, 129.82, 180.36,…, indicate the crystallisation temperature in °C. For the figures in the second row seen overlapped in the bottom chart (the degree of crystallinity at maximum dx/dt), see Table 6.

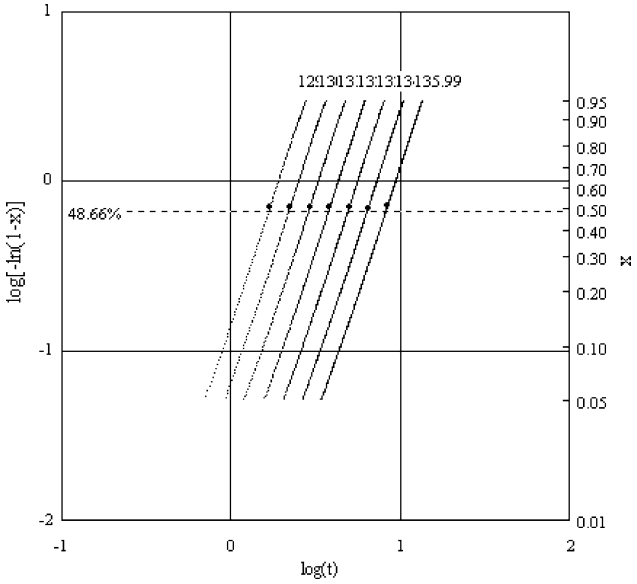

Fig. 9. Plot of isothermal crystallisation data of PP-SP in accordance with Eq. (12). The unit of time, t, is minute. The figures to show the crystallisation temperature overlapped in this computer output are 129.8, 130.9, 131.9, 132.9, 133.9, 135.0 and 136.0 °C.

or to errors caused by the method for extrapolating the sets of data in Fig. 10.

The slope of lines in Fig. 10 gives the combined free-energy, $\sigma_e\sigma_s = 8.77 \pm 2.11 \times 10^{-4}$ J^2/m^4, with $b = 6.65 \times 10^{-10}$ m and $\Delta H_u = 1.99 \times 10^8$ J/m^{-3} (Kamide [8]). That the growth process may well be affected by the nature of primary nucleus was found earlier in the study on the combination of polypropylene and a graphite fibre, in which isothermal crystallisation was conducted at 10–11 different temperatures and $\sigma_e\sigma_s = 1.032$ and 0.628×10^{-3} J^2/m^4 for

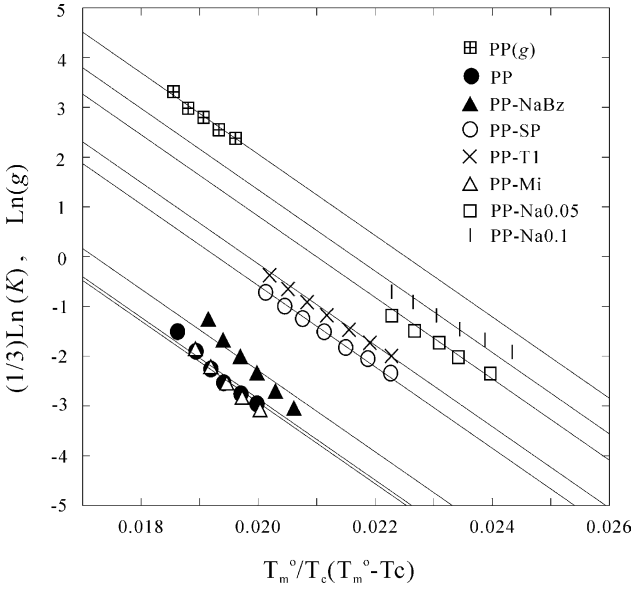

Fig. 10. Plot of (1/3)ln(K) and ln(g) vs. $T_c\Delta T$.

Table 6
The results of fitting to the Avrami–Evans equation

Sample	T_c (°C)	Peak X (%)	n	K
PP (neat)	124.3	44.50	2.661±0.006	1.41×10^{-2}
	125.3	46.09	2.814±0.007	4.61×10^{-3}
	126.3	46.17	2.935±0.009	1.52×10^{-3}
	127.3	46.36	2.927±0.008	7.01×10^{-4}
	128.3	46.64	2.878±0.007	3.53×10^{-4}
	129.3	46.01	2.797±0.009	1.94×10^{-4}
PP-NaBz	126.3	45.05	3.009±0.032	2.34×10^{-2}
	127.3	45.54	3.002±0.023	7.08×10^{-3}
	128.3	46.42	2.999±0.015	2.66×10^{-3}
	129.3	47.69	3.005±0.011	1.00×10^{-3}
	130.3	48.24	3.001±0.009	3.63×10^{-4}
	131.3	49.25	2.997±0.008	1.35×10^{-4}
PP-SP	129.8	50.12	3.002±0.006	1.41×10^{-1}
	130.9	50.81	3.003±0.007	6.25×10^{-2}
	131.9	50.34	3.006±0.007	2.73×10^{-2}
	132.9	50.46	2.998±0.007	1.25×10^{-2}
	133.9	50.81	3.005±0.008	5.64×10^{-3}
	135.0	50.04	3.002±0.008	2.59×10^{-3}
	136.0	51.19	3.002±0.008	1.21×10^{-3}
PP-T1	130.0	51.36	2.999±0.011	3.81×10^{-1}
	131.0	51.22	3.006±0.009	1.82×10^{-1}
	132.0	51.85	2.999±0.010	8.20×10^{-2}
	133.0	51.46	3.000±0.011	3.60×10^{-2}
	134.1	51.62	2.998±0.011	1.57×10^{-2}
	135.1	51.26	3.001±0.012	7.06×10^{-3}
	136.1	51.64	3.001±0.012	3.24×10^{-3}
PP-Mi	125.5	49.89	2.986±0.008	4.38×10^{-3}
	126.5	48.65	3.004±0.007	1.49×10^{-3}
	127.5	47.48	2.995±0.008	5.87×10^{-4}
	128.5	47.23	2.959±0.009	2.60×10^{-4}
	129.5	45.10	2.904±0.009	1.15×10^{-4}
PP-NA0.05	136.1	48.05	2.949±0.010	3.62×10^{-2}
	137.1	47.69	2.983±0.011	1.49×10^{-2}
	138.1	48.00	3.002±0.009	6.36×10^{-3}
	139.0	48.22	2.997±0.008	2.94×10^{-3}
	140.0	48.27	2.999±0.007	1.43×10^{-3}
PP-NA0.1	136.0	47.89	2.931±0.024	1.62×10^{-1}
	137.0	47.65	3.005±0.023	6.97×10^{-2}
	138.0	47.93	2.996±0.020	3.52×10^{-2}
	138.9	47.16	2.998±0.021	1.68×10^{-2}
	139.9	48.28	2.998±0.021	8.30×10^{-3}
	140.9	47.16	3.005±0.019	4.09×10^{-3}

The general form of Avrami–Evans equation: $\log[-\ln(1-X)]=\log K+n\log t$. Theoretically, n should be 3 in the present case.

the neat polymer and the mixture, respectively (Watanabe and Iguchi [1]). For the data of the present study, detailed arguments should be suspended as the number of data for each sample were insufficient.

Table 7
The densities of nucleator particles and the actual nuclei

Sample	N (cm^{-3})	C (cm^{-3})	N/C
PP	–	1.07×10^{5}	–
PP-NaBz	3.91×10^{7}	5.25×10^{5}	7.45×10^{2}
PP-SP	1.32×10^{8}	1.35×10^{8}	9.78×10^{-1}
PP-T1	8.76×10^{10}	4.31×10^{8}	2.03×10^{2}
PP-Mi	2.74×10^{8}	1.07×10^{5}	2.56×10^{3}
PP-Na0.05	6.80×10^{9}	3.94×10^{9}	1.73×10^{0}
PP-Na0.1	1.36×10^{10}	1.97×10^{10}	6.90×10^{-1}

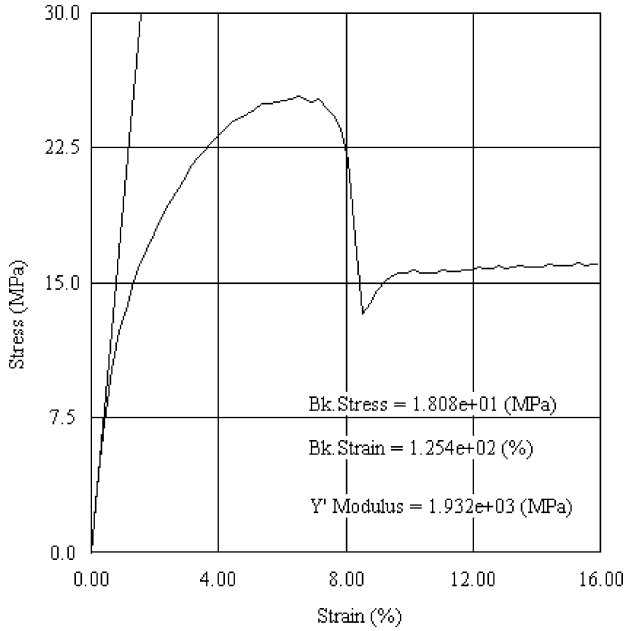

Fig. 11. An example of stress–strain curve. Sample: PP (neat). The initial slope was drawn with an aid of a computer programme.

3.5. The effect of the nucleators on the mechanical properties

The stress–strain curves showed a typical shape characteristic to unoriented crystalline polymers, as an example is shown in Fig. 11, in that the stress reached a maximum at 2–6% strain, fell down and stayed at a certain level until the specimens breaks. The values of Young's modulus obtained from the initial slopes are listed in Table 8 along with the strain and stress at the maximum.

When plotted against the logarithm of the nucleus density as in Table 7, the points aligned on a straight line, showing that the larger the density of nucleus, the larger the Young's modulus, without regards to the kind of nucleator applied, as in Fig. 12. This tendency is in accordance with the result in a recently published paper (Gui et al. [6]) in which the Young's modulus and some other mechanical characteristics of polypropylene containing various amount of another organophosphate compound (Na-40) were plotted against the nucleus density obtained by an different method. The strain and the stress at the maximum showed a tendency to decrease with C as seen in Fig. 13.

Table 8
Young's modulus, strains and strains at maximum, of film specimens

Sample	Young's modulus (GPa)	Strain at maximum (%)	Stress at maximum (MPa)
PP	1.62±0.08	5.97±1.59	22.18±4.10
PP-NaBz	1.67±0.03	7.53±0.60	21.85±2.43
PP-SP	1.79±0.06	5.05±1.69	17.31±2.71
PPT1	1.81±0.03	4.36±1.27	15.65±1.43
PP-Mi	1.61±0.11	5.30±1.29	16.63±3.06
PP-Na0.05	1.87±0.08	5.00±1.81	16.90±1.80
PP-Na0.1	1.91±0.05	2.43±0.15	14.20±0.34

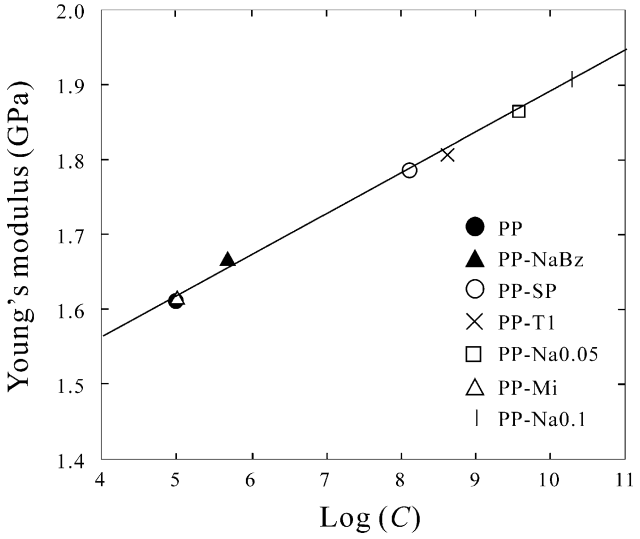

Fig. 12. Young's modulus of various polymer–nucleator mixtures plotted vs. log(C) (the dimension of C, cm^{-3}).

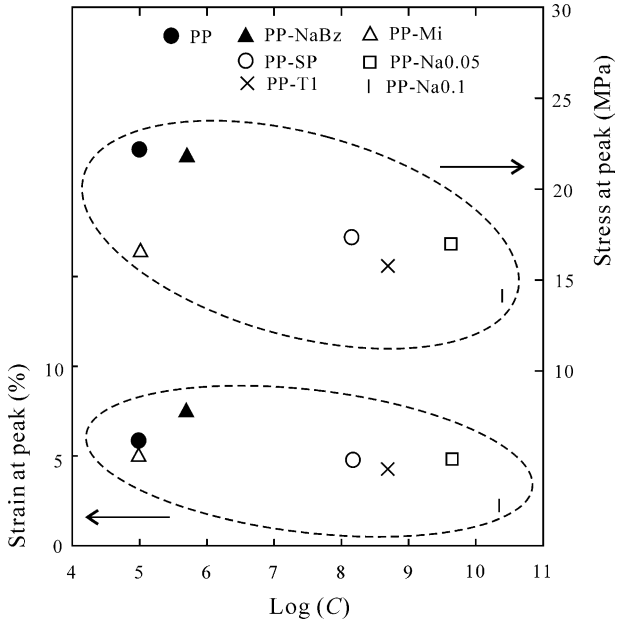

Fig. 13. Strain and the stress at maximum plotted vs. log(C) (the dimension of C, cm^{-3}).

The fact that the mechanical properties are correlated to the nucleus density without regard to the chemical structure of nucleators is interesting but argument can hardly be furthered without detailed knowledge about the inside and the boundaries of spherulites. It should at least be certain that nucleator particles used in such a small amount as less than one percent did not have any significance for directly modifying the mechanical properties, not as in the case of composite materials in which the effect of fillers would become distinct when the content exceeded several percent.

4. Conclusion

For the crystallisation of polypropylene containing various substances as nucleators, it was demonstrated that a free-energy parameter obtained from DSC traces under various cooling rates could be a measure to evaluate the effectiveness for forming the primary nucleus. Among the substances studied, the parameter of organophosphate compound (NA-11) was the lowest, whilst those of sodium benzoate and a sorbitol derivative (Millad 3988) were larger and rather close to that of the 'natural' nucleator existed in the neat polymer. The values of fine and course graphite particles (T1 and SP-270) were almost the same, and intermediate.

The actual nucleus density in the polymer was estimated from the radial growth rate of spherulite and the bulk growth rate, the latter obtained by the analysis of crystallisation isotherms. It was interpreted that the dispersibility of NA-11 and the fine graphite powders was good, whereas Millad 3988, SP-270 and sodium benzoate tended to form large clusters.

The Young's modulei of film specimens increased linearly with the logarithm of the nucleus density, suggesting that mechanical properties of nucleator-added polypropylene did not depend on the chemical structure of nucleators but on the increase of primary nuclei that changed the fine structure of the crystallised polymer.

Acknowledgements

The authors thank Dr N. Kawamoto, Asahi Denka Co. Ltd, and Mr K. Tsukamoto, Nippon Graphite Industries, Ltd, for kindly supplying the organic nucleating agents and the graphite powders, respectively.

References

[1] Watanabe Y, Iguchi M. Proceedings of 1978 annual conference of research institute of polymers and textiles, Tsukuba 1978 p. 117.
[2] Iguchi M, Watanabe Y. Br Polym J 1977;9:251.
[3] Iguchi M, Watanabe Y. Polym Prepr Jpn 1978;27:499.
[4] Feng Y, Jin X, Hay N. J Appl Polym Sci 1998;69:2089.
[5] Kim YC, Kim YK. Polym Eng Sci 1991;31:14.
[6] Gui Q, Xin Z, Zhu W, Dai G. J Appl Polym Sci 2003;88:297.
[7] Mandelkern L. Crystallization of polymers. New York: McGraw-Hill; 1964.
[8] Burns JR, Turnbull D. J Appl Phys 1966;37:4201.
[9] Kamide K. Kobunshi Kagaku 1968;25:532.
[10] Banks W, Gordon M, Sharples A, Hay JN. J Polym Sci 1964;2:4095.
[11] Hillier IH. Polymer 1968;9:19.
[12] Danusso F, Tieghi G, Ferderer V. Eur Polym J 1970;6:1521.
[13] (a) Avrami M. J Chem Phys 1939;7:1103.
(b) Avrami M. J Chem Phys 1940;8:212.
(c) Avrami M. J Chem Phys 1941;9:117.
[14] Evans UR. Trans Faraday Soc 1945;41:365.
[15] Kamide K, Fujii K. Kobunshi Kagaku 1968;25:155.